*To be published in Optics Letters:*

| | |
|---|---|
| **Title:** | Lensless ghost imaging with sunlight |
| **Authors:** | Ling-An Wu, Guang-Jie Zhai, Xue-Feng Liu, Xi-Hao Chen, Xu-Ri Yao, and Wen-Kai Yu |
| **Accepted:** | 26 February 2014 |
| **Posted:** | 26 February 2014 |
| **Doc. ID:** | 202752 |

# Lensless ghost imaging with sunlight

**Xue-Feng Liu,[1] Xi-Hao Chen,[1,2] Xu-Ri Yao,[1] Wen-Kai Yu,[1] Guang-Jie Zhai[1,*] and Ling-An Wu[3,†]**

[1] *Key Laboratory of Electronics and Information Technology for Space Systems, Center for Space Science and Applied Research, Chinese Academy of Sciences, Beijing 100190, China*

[2] *College of Physics, Liaoning University, Shenyang 110036, China*

[3] *Laboratory of Optical Physics, Institute of Physics and Beijing National Laboratory for Condensed Matter Physics, Chinese Academy of Sciences, Beijing 100190, China*

[*] *gjzhai@nssc.ac.cn*

[†] *wula@aphy.iphy.ac.cn*

Compiled February 25, 2014

Lensless ghost imaging with sunlight is demonstrated, for the first time to our knowledge. A narrow spectral line is first filtered out and its intensity correlation measured. With this true thermal light source, an object consisting of two holes is imaged. The realization of lensless ghost imaging with sunlight is a step forward towards the practical application of ghost imaging with ordinary daylight as the source of illumination. 

*OCIS codes:* 110.2970, 030.5260, 030.5290.



Imaging is one of the most familiar phenomena in optics. In traditional imaging, a detector with spatial resolution is needed to detect the signal and record the image of an object. In 1995, Shih's group first demonstrated a new type of imaging called ghost imaging (GI), in which only a single-pixel detector or a bucket detector is needed to collect the light from the object, while a detector with spatial resolution called the reference detector is used to collect information about the source [1]. At first, GI was performed with entangled photons as the source and was considered as a characteristic of entanglement, but it was found later that GI can also be achieved with thermal light, the earliest experiments being based on pseudothermal light generated by a laser passing through a rotating ground glass plate [2-5]. The first demonstration of GI with true thermal light was achieved by Wu's group, in which the source was a hollow-cathode lamp [6].

One of the differences between GI with entangled light and thermal light is that the latter can be used to realize lensless imaging [7-11]. As in thermal light GI, only a single-pixel detector is needed to collect the object information without any imaging lens, which makes the imaging setup much simpler and more adaptable. Therefore, thermal light GI has been widely demonstrated in fields such as fluorescence imaging [12], lidar detection [13] and optical coherence tomography [14]. However, until now both the experiments of GI with pseudothermal and true thermal light were realized with man-made light sources; achieving GI with naturally occurring light will have enormous value in real applications. We report here the first demonstration, to our knowledge, of lensless GI with sunlight, the most common natural light source.

In the first experiment measuring the intensity correlation of thermal light performed by Hanbury Brown and Twiss (HBT) [15, 16], it was found that only when the coherence time of the light field is close to, or longer than the time resolution of the detector, can the intensity correlation be observed. To obtain a source with a sufficiently long coherence time, we employ a Faraday anomalous dispersion optical filter (FADOF) to filter the sunlight down to a narrow spectral width. The filter setup is shown in Fig. 1. Glan1 and Glan2 are two Glan prisms with an extinction ratio of $10^{-5}$; the FADOF rotates the polarization of light at its resonant wavelength by 90° through Faraday anomalous dispersion, so with the correct orientation of Glan2 all other wavelengths are filtered out. Our FADOF (made by the Wuhan Institute of Physics and Mathematics, Chinese Academy of Sciences) has a resonant wavelength $\lambda$ at the 780 nm transition of Rb, with a bandwidth of 0.01 nm and peak transmission of about 0.5. Due to nonuniformity of the magnetic field in the FADOF, which leads to depolarization as well as widening of the transmitted light linewidth, a small quantity of light outside the expected wavelength range will leak from the filter system. To decrease the noise caused by the leakage, an interference filter IF with a transmission wavelength centered at 780 nm is used to prefilter the light in front of the system. The bandwidth of the filter is 3 nm and the peak transmission about 0.98. With this setup, we obtain a 780 nm beam of sunlight with a bandwidth close to 0.01 nm.

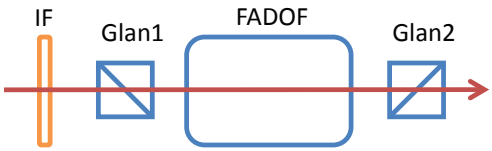


Fig. 1. Narrow band filter setup. IF, interference filter; Glan1, Glan2, Glan prisms; FADOF, Faraday anomalous dispersion optical filter.

To check the performance of the FADOF, we first carried out an HBT experiment, with the setup shown in Fig. 2. The sunlight is collected by a Meade 127ED astronomical telescope which can automatically track the sun. An absorption type red glass filter is fitted to the telescope objective to block out most of the spectrum far away from 780 nm. The remaining light around 780 nm is transmitted in a multi-mode fiber to an optical table, where it is collimated by a fiber collimator C0 and focused by a lens L of focal length $f$=10 cm to a spot of diameter $d$=0.75 mm in the center of the FADOF. This focal point acts as a secondary source S of thermal light. The beam is then divided by a 50:50 beamsplitter, and the transmitted and reflected beams are coupled through fiber collimators C1 and C2 of diameters 10mm into two single-photon detectors (Perkin Elmer SPCM-AQRH-13-FC) APD1 and APD2, respectively. The distances from the source S to the collimators are both $z$=31 cm, so the spatial coherence length at the planes of the collimators is

$$l_c = \frac{\lambda z}{d} = 0.32\text{mm}. \quad (1)$$

To ensure that the sunlight collected by the two detectors have corresponding coherence areas we insert two pinholes of diameter 0.3 mm in front of the two collimators at the corresponding transverse positions. The detector counts are sent to a time-correlated single-photon counting module (Becker & Hickl SPC-130) and processed in a computer. From the coincidence counts at different arrival times of the photons at the two detectors we can derive the coherence time of the filtered 780 nm sunlight.

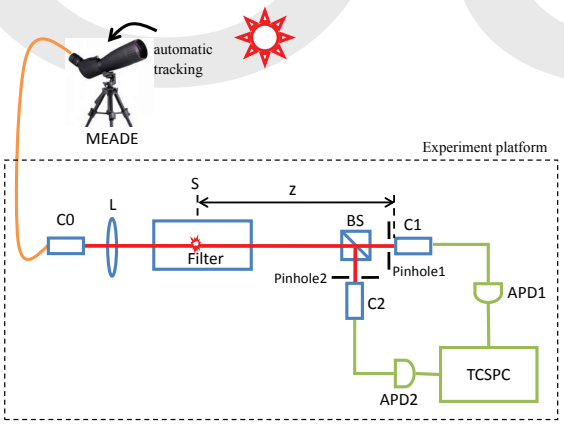


Fig. 2. Experimental setup of HBT measurement of sunlight. MEADE, Meade astronomical telescope; Filter, FADOF setup of Fig. 1; BS, 50:50 beamsplitter; C1, C2, fiber collimators; TCSPC, time-correlated single-photon counting module. The distances from the secondary source S to the collimators are both $z$=31 cm.

The HBT measurement results are plotted in Fig. 3, which shows the coincidence counts $C(\Delta t)$ as a function of the difference in time-of-arrival $\Delta t$ of photons at the two detectors. The peak at $\Delta t = 0$ reveals the intensity correlation of the narrowband sunlight. We see that the full-width-at-half-max (FWHM) of the peak is 1.1 ns, which is much wider than our theoretical estimate of the coherence time of 780 nm light with a bandwidth of 0.01 nm:

$$\tau_c = \frac{1}{\Delta\nu} = \frac{\lambda^2}{c\Delta\lambda} = 0.2\text{ns}, \quad (2)$$

where $\Delta\nu$ is the frequency bandwidth and $c$ the velocity of light. The reason for this is that the time resolution of our detection system, including the single-photon detectors and TCSPC module, is about 0.45 ns and so is longer than the coherence time.

The intensity correlation function $g^{(2)}(\Delta t = 0)$ of the light on the two collimators can be defined as [6]:

$$g^{(2)}(\Delta t = 0) = \frac{C(\Delta t = 0)}{C(\Delta t \to \infty)}. \quad (3)$$

in which $C(\Delta t = 0)$ can be obtained from the Gaussian fit directly, and $C(\Delta t \to \infty)$ is chosen as the background of the Gaussian fit. From Eq. (3), the value of $g^{(2)}(\Delta t = 0)$ is calculated to be 1.04, much less than the theoretical value of 2 for true thermal light. The main reason is again the relatively long time resolution of the detection system. Other reasons include the additional background noise caused by the leakage of the filter system, and incomplete overlap of the coherent areas at the detectors due to possible misalignment. Nevertheless, the observation of a correlation peak proves that we are able to measure the intensity correlation of narrowband sunlight, which is a necessary condition for realizing GI with pure sunlight.

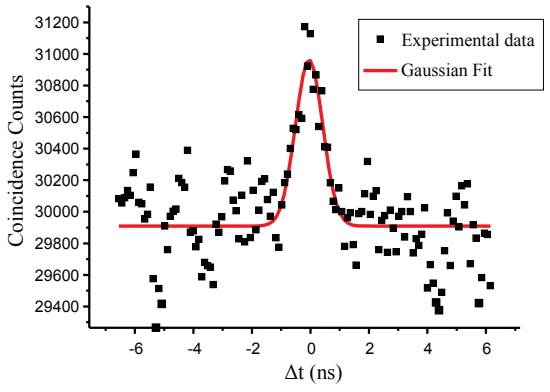


Fig. 3. Coincidence counts as a function of the arrival-time difference between photons at the two detectors. Black squares, experimental data. Solid curve, Gaussian fit.

The HBT experimental setup was then modified to perform lensless GI with sunlight, as shown in Fig. 4. Pinhole 2 in the reflected beam of Fig. 2 is replaced by an

object Obj, behind which a lens L2 focuses the light passing through the object into the single photon detector APD2. It should be emphasized that the lens here does not provide the function of imaging, but just collects the photons passing through the object to the collimator, which has no spatial resolution. To image the object, the collimator C1 is scanned in the direction transverse to the beam, and the coincidence counts of the detectors are recorded as a function of the transverse distance $x$.

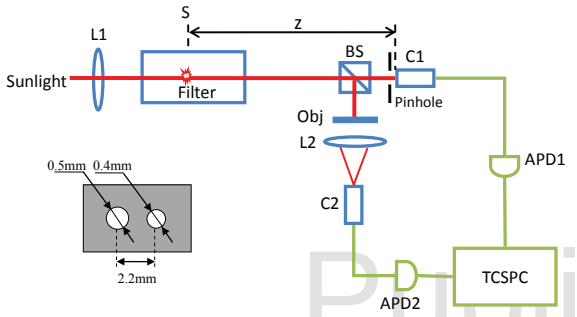


Fig. 4. Experimental setup of lensless GI with sunlight. Sunlight is collected by the Meade astronomical telescope and multi-mode fiber as in the HBT experiment. BS, 50:50 beamsplitter. Obj, object shown in bottom left, consisting of a mask with two holes. The distances from the secondary source S to the collimator and object are both $z$=31 cm.

The object in our experiment is a mask consisting of two round holes, 2.2 mm apart, as shown in the bottom left of Fig. 4. It was made by sticking a needle into a piece of copper foil, so the two holes had unequal diameters of approximately 0.5 mm and 0.4 mm. The one-dimensional ghost image of a horizontal cross-section of the object was obtained from the second-order intensity correlation function $g^{(2)}(x)$

$$g^{(2)}(x) = \frac{C(x, \Delta t = 0)}{C(x, \Delta t \to \infty)} \tag{4}$$

and is plotted in Fig. 5. The black points were calculated from the experimental data, while the red line is a Gaussian fit. The FWHMs of the two peaks are 0.89 mm and 0.71 mm, respectively. Because the spatial coherence length at the detection plane is 0.32 mm, which is close to the real sizes of the holes, the diameters could not be measured precisely, but the distance between the two peaks is 2.2 mm, which is exactly the distance between the two holes. It should be noted that the visibility of the image is only 1.2%, again restricted mainly by the limited time resolution of the detection system and the leakage of the filter system.

Among the reasons for the low visibility in our experiment, the most crucial physical restriction is the relatively short coherence time of the source and the limited time resolution of the detection system. This problem is a major difficulty in GI with sunlight, and needs to be

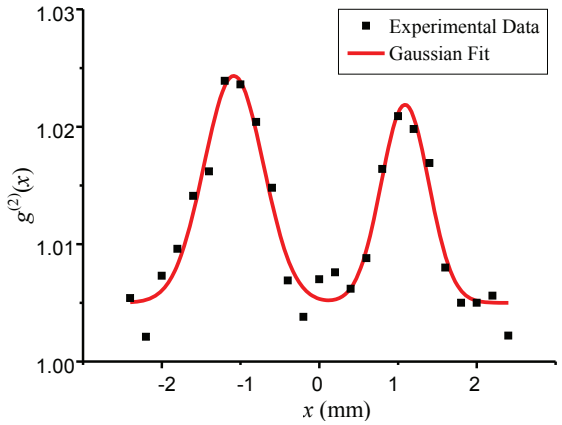


Fig. 5. Lensless GI image of the two-hole mask illuminated with sunlight. Horizontal axis: distance $x$ scanned by collimator C1. Vertical axis: intensity correlation function $g^{(2)}(x)$. Black points, experimental data. Solid curve, Gaussian fit.

solved in future work. Below, we analyze the influences of coherence time and time resolution on the intensity correlation function. In real applications, the filters used in the two arms may not have exactly the same specifications, which will cause some difference between the bandwidths of the light incident on the two detectors. The relation between the intensity correlation function and coherence time of light in the two arms can be expressed as

$$g^{(2)}\left(\Delta t = 0\right) = 1 + \frac{2\tau_{c1}\tau_{c2}}{\sqrt{\tau_{c1}^2 + \tau_{c2}^2}\sqrt{\tau_{c1}^2 + \tau_{c2}^2 + t_r^2}} \tag{5}$$

where $t_r$ is the effective time resolution of the detection system, and

$$\tau_{c1} = \frac{\lambda^2}{c\Delta\lambda_1}, \ \tau_{c2} = \frac{\lambda^2}{c\Delta\lambda_2}. \tag{6}$$

Here $\tau_{c1}$, $\tau_{c2}$ are the coherence times and $\Delta\lambda_1$, $\Delta\lambda_2$ the bandwidths of the light at the reference and bucket detectors, respectively.

In Fig. 6 the dependence of the intensity correlation function on the filter bandwidths is plotted. The time resolution $t_r$ is assumed to be 450 ps, as determined by the single-photon detector in our experiment. From the figure it is clear that the narrower the linewidth, the higher the intensity correlation function will be. If the linewidths of the two light beams were both 0.001 nm, then the corresponding coherence times would both be 2 ns and the intensity correlation function would be 1.99, almost reaching the theoretical value. However, for bandwidths of 0.05 nm, the coherence times are both 0.04 ns, much less than the time resolution 0.45 ns, then the intensity correlation function is only 1.13. Additionally, we notice that only when the bandwidths of both arms are sufficiently narrow can a large intensity correlation be obtained. If only one arm has a narrow bandwidth while

the other is too broad, the intensity correlation will still be very small. For example, when the bandwidth in one arm is 0.01 nm (as in our experiment) but the other is as large as 0.05 nm, the intensity correlation function is only 1.16. This means that the bandwidths in both arms must be sufficiently narrow to obtain a good ghost image.

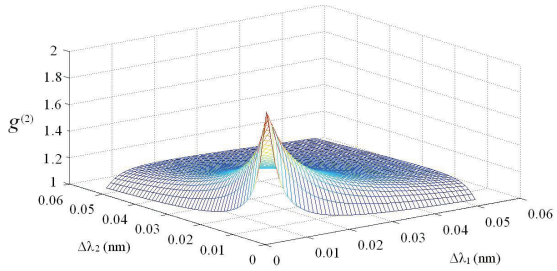


Fig. 6. Dependence of the intensity correlation function on the filter bandwidths. The time resolution $t_r$ of the detection system is taken as 450 ps.

In conclusion, we have performed a proof-of-principle experiment demonstrating lensless GI with pure filtered sunlight. Although the image visibility is low, it can be increased by selecting a filter with an even narrower spectral width and less noise leakage, for example, by using a high finesse Fabry-Perot filter. As the sun is a free and universally available source of illumination, and GI only needs a single-pixel detector to obtain information about the object without an imaging lens, GI with sunlight has wide applications in situations where the direct observation of a target with imaging resolution is difficult.

This work was supported by the National Basic Research Program of China (Grant No. 2010CB922904), the National Natural Science Foundation of China (Grant Nos. 60978002, 61274024, 11375224 and 11204117), the Hi-Tech Research and Development Program of China (Grant No. 2011AA120102), the National Major Scientific Instruments Development Project of China (Grant No. 2013YQ030595), and the China Postdoctor Science Foundation (Grant No. 2013M540146).

## References

1. T. B. Pittman, Y. H. Shih, D. V. Strekalov, and A. V. Sergienko, Phys. Rev. A **52**, R3429 (1995).
2. R. S. Bennink, S. J. Bentley, and R. W. Boyd, Phys. Rev. Lett. **92**, 033601 (2004).
3. A. Gatti, E. Brambilla, M. Bache, and L. A. Lugiato, Phys. Rev. Lett. **93**, 093602 (2004).
4. A. Valencia, G. Scarcelli, M. D. Angelo, and Y. H. Shih, Phys. Rev. Lett. **94**, 063601 (2005).
5. A. Gatti, M. Bache, D. Magatti, E. Brambilla, F. Ferri and L. A. Lugiato, J. Mod. Opt. **53,** 739 (2006).
6. D. Zhang, Y. H. Zhai, and L. A. Wu, Opt. Lett. **30**, 2354 (2005).
7. J. Cheng and S. S. Han, Phys. Rev. Lett. **92**, 093903 (2004).
8. D. Z. Cao, J. Xiong, and K. G. Wang, Phys. Rev. A **71**, 013801 (2005).
9. G. Scarcelli, V. Berardi, and Y. H. Shih, Appl. Phys. Lett. **88**, 061106 (2006).
10. L. Basano and P. Ottonello, Appl. Phys. Lett. **89**, 091109 (2006).
11. X. H. Chen, Q. Liu, K. H. Luo, and L. A. Wu, Opt. Lett. **34**, 695 (2009).
12. N. Tian, Q. C. Guo, A. L. Wang, D. L. Xu, and L. Fu, Opt. Lett. **36**, 3302 (2011).
13. C. Q. Zhao, W. L. Gong, M. L. Chen, E. R. Li, H. Wang, W. D. Xu, and S. S. Han, Appl. Phys. Lett. **101,** 141123 (2012).
14. X. F. Liu, X. R. Yao, X. H. Chen, L. A. Wu, and G. J. Zhai, J. Opt. Soc. Am. A **29**, 1922 (2012).
15. R. H. Brown and R. Q. Twiss, Nature **177**, 27 (1956).
16. R. H. Brown and R. Q. Twiss, Nature **178**, 1046 (1956).

## Informational Fourth Page

In this section, please provide full versions of citations to assist reviewers and editors (OL publishes a short form of citations) or any other information that would aid the peer-review process.

## References


1. T. B. Pittman, Y. H. Shih, D. V. Strekalov, and A. V. Sergienko, "Optical imaging by means of two-photon quantum entanglement," Phys. Rev. A **52**, R3429 (1995).
2. R. S. Bennink, S. J. Bentley, and R. W. Boyd, "Quantum and classical coincidence imaging", Phys. Rev. Lett. **92**, 033601 (2004).
3. A. Gatti, M. Bache, D. Magatti, E. Brambilla, F. Ferri and L. A. Lugiato, "Coherent imaging with pseudo-thermal incoherent light", J. Mod. Opt. **53,** 739 (2006).
4. A. Gatti, E. Brambilla, M. Bache, and L. A. Lugiato, "Ghost Imaging with Thermal Light: Comparing Entanglement and Classical Correlation", Phys. Rev. Lett. **93**, 093602 (2004).
5. A. Valencia, G. Scarcelli, M. D. Angelo, and Y. H. Shih, "Two-Photon Imaging with Thermal Light", Phys. Rev. Lett. **94**, 063601 (2005).
6. D. Zhang, Y. H. Zhai, and L. A. Wu, "Correlated two-photon imaging with true thermal light", Opt. Lett. **30**, 2354 (2005).
7. J. Cheng and S. S. Han, "Incoherent Coincidence Imaging and Its Applicability in X-ray Diffraction", Phys. Rev. Lett. **92**, 093903 (2004).
8. D. Z. Cao, J. Xiong, and K. G. Wang, "Geometrical optics in correlated imaging systems", Phys. Rev. A **71**, 013801 (2005).
9. G. Scarcelli, V. Berardi, and Y. H. Shih, "Phase-conjugate mirror via two-photon thermal light imaging", Appl. Phys. Lett. **88,** 061106 (2006).
10. L. Basano and P. Ottonello, "Experiment in lensless ghost imaging with thermal light", Appl. Phys. Lett. **89**, 091109 (2006).
11. X. H. Chen, Q. Liu, K. H. Luo, and L. A. Wu, "Lensless ghost imaging with true thermal light", Opt. Lett. **34**, 695 (2009).
12. N. Tian, Q. C. Guo, A. L. Wang, D. L. Xu, and L. Fu, "Fluorescence ghost imaging with pseudothermal light", Opt. Lett. **36**, 3302 (2011).
13. C. Q. Zhao, W. L. Gong, M. L. Chen, E. R. Li, H. Wang, W. D. Xu, and S. S. Han, "Ghost imaging lidar via sparsity constraints", Appl. Phys. Lett. **101**, 141123 (2012).
14. X. F. Liu, X. R. Yao, X. H. Chen, L. A. Wu, and G. J. Zhai, "Thermal light optical coherence tomography for transmissive objects", J. Opt. Soc. Am. A **29**, 1922 (2012).
15. R. H. Brown and R. Q. Twiss, "Correlation between photons in two coherent beams of light", Nature **177**, 27 (1956).
16. R. H. Brown and R. Q. Twiss, "A test of a new type of stellar interferometer on Sirius", Nature **178**, 1046 (1956).